

X-ray Synchrotron Study of Packing and Protrusions of Polymer–Lipid Monolayers at the Air–Water Interface

J. Majewski,^{†,¶} T. L. Kuhl,[‡] K. Kjaer,[§] M. C. Gerstenberg,[§] J. Als-Nielsen,[⊥]
J. N. Israelachvili,[‡] and G. S. Smith^{*,†}

Contribution from the Manuel Lujan Neutron Scattering Center, Los Alamos National Laboratory, Los Alamos, New Mexico 87545, Department of Solid State Physics, Risø National Laboratory, DK-4000 Roskilde, Denmark, Niels Bohr Institute, H. C. Ørsted Laboratory, Copenhagen University, Denmark, and Materials Research Laboratory, University of California, Santa Barbara, California 93106

Received August 27, 1997

Abstract: Using X-ray scattering, the structure of compressed phospholipid monolayers at the air–water interface matrixed with varying amounts of polymer lipid has been determined. The out-of-plane structure of the monolayer was greatly perturbed by the incorporation of the bulky polymer lipid resulting in a systematic roughening of the interface and a decrease in the coherently Bragg-scattering lipid tail region. Our results indicate that the increased lateral packing stresses due to the hydrophilic polymer chains are predominately relaxed through an increase in lipid protrusions rather than an increased area per lipid molecule.

Biological cells and extracellular matrixes contain a variety of macromolecular structures separated by an aqueous phase. Both specific and nonspecific interactions between these hydrated macromolecules play critical roles in a variety of biological processes. One of the most simplified models for biological membranes is lipid monolayers at the air–water interface and much structural data has been obtained from such systems using a variety of methods, recently including X-ray specular reflection and diffraction.¹ A more difficult area to probe has proven to be the dynamic motions of such hydrophilic/hydrophobic assemblies and their constituent molecules and submolecular groups.

One way to increase the applicability of a lipid monolayer to model a membrane with an extracellular matrix is to incorporate lipids which expose hydrophilic polymers to the aqueous phase—the so-called polymer lipids, which have received much recent attention due to their application in drug delivery.² The polymer lipid is generally a phosphatidyl ethanolamine of varying tail length with poly(ethylene glycol) (PEG or EO_n of varying *n*) chemically grafted to the terminal amine of the headgroup. Since PEG is a water-soluble polymer, it also acts as an enlarged hydrophilic headgroup when it is chemically bound to the lipid headgroup. These polymer-modified lipids also serve as good models for terminally grafted

polymers of low MW, where the “grafting” density of the polymer chains can be varied and quantitatively controlled by simply varying the ratio of unmodified to polymer-modified lipid within a mixed monolayer or bilayer.^{3,4}

Such a system is particularly interesting for probing the effects of hydrophilic headgroup interactions on the dynamics and structure of lipid assemblies. Repulsive “hydration” forces are believed to be important for determining the molecular packing in monolayers and bilayers, and at short range can dominate the van der Waals and electrostatic interactions between opposing bilayers. Through a large body of experimental work, hydration forces, which typically have a range of 10–30 Å, have been found to decay roughly exponentially with a characteristic decay length of 1–3 Å.⁵ Although this functional form of the repulsive interaction is well accepted, the source of this repulsion has remained controversial with some arguing that it is due to solvent (water) structure extending from the surface,⁵ while others have proposed that it is an entropic or osmotic force resulting from the fluctuations of protruding surface groups, e.g., lipids that protrude from the liquid-like membrane surface and interact directly with each other.⁶

Although the “hydration” force is generally associated with normal interactions between two opposing lipid surfaces, the same interactions also occur laterally within the plane of a single lipid surface layer.⁷ Thus, more highly hydrated lipids would be expected to have larger lateral repulsive interactions with neighboring lipids compared to less hydrated lipids. Similarly,

* To whom correspondence should be addressed.

† Los Alamos National Laboratory.

‡ University of California, Santa Barbara.

§ Risø National Laboratory.

⊥ Copenhagen University.

¶ On leave from the Institute of Physics, Polish Academy of Sciences.

(1) Als-Nielsen, J.; Jacquemain, D.; Kjaer, K.; Lahav, M.; Leveiller, F.; Leiserowitz, L. *Phys. Rep.* **1994**, *246*, 251. Als-Nielsen, J.; Kjaer, K. X-ray Reflectivity and Diffraction Studies of Liquid Surfaces and Surfactant Monolayers. In *The Proceedings of the NATO Advanced Study Institute, Phase Transitions in Soft Condensed Matter*; Riste, T., Sherrington, D., Ed.; Geilo, Norway, April 4–14, 1989; Plenum Publishing Corp.: New York, 1989; pp 113–137. Kjaer, K. *Physica B* **1994**, *198*, 100. Proceedings of the 3rd International Conference on Surface X-ray and Neutron Scattering, Dubna, Russia, June 24–29, 1993.

(2) Lasic, D., Martin, F., Eds. *Stealth Liposomes*; CRC Press: Boca Raton, 1995; p 289 for a complete review.

(3) Kuhl, T.; Leckband, D.; Lasic, D.; Israelachvili, J. *Biophys. J.* **1994**, *66*, 1479.

(4) Kenworthy, A. K.; Hristova, K.; Needham, D.; McIntosh, T. J. *Biophys. J.* **1995**, *68*, 1921.

(5) Leikin, S.; Parsegian, V. A.; Rau, D. C.; Rand, R. P. *Annu. Rev. Phys. Chem.* **1993**, *44*, 369. McIntosh, T. J.; Simon, S. A. *Annu. Rev. Biophys. Biomol. Struct.* **1994**, *23*, 27.

(6) Israelachvili, J.; Wennerstrom, H. *J. Phys. Chem.* **1992**, *96*, 520. Wiener, M. C.; White, S. H. *Biophys. J.* **1992**, *61*, 434.

(7) Naumann, C.; Brumm, T.; Rennie, A. R.; Penfold, J.; Bayerl, T. M. *Langmuir* **1995**, *11*, 3948. Naumann, C.; Dietrich, C.; Lu, J. R.; Thomas, R. K.; Rennie, A. R.; Penfold, J.; Bayerl, T. M. *Langmuir* **1994**, *10*, 1919.

an increase of entropic fluctuations would lead to larger repulsive interactions between adjacent headgroups and greater out-of-plane protrusions.⁸

To gain insight into the types of physical properties discussed above, a series of X-ray reflection and grazing incidence diffraction (GID) experiments were performed on lipid monolayers composed of distearoyl phosphatidyl ethanolamine (DSPE) matrixed with 0, 1.3, or 9.0% of the same lipid with poly(ethylene glycol) chains (PEG, 2000 MW) covalently linked to its headgroup, thereby forming DSPE-PEG. The use of the novel molecule DSPE-PEG is especially suitable for probing the relative contributions of lipid hydration versus entropic protrusions, since this molecule has an extremely large hydrophilic headgroup but still forms stable monolayers at the air-water interface.⁹ Additionally, this system is also a suitable model for studying short chain, end-grafted polymer layers.¹⁰

The GID and reflectivity experiments were performed at the BW1 (wiggler) beam line at the HASYLAB synchrotron source (Hamburg, Germany) using the liquid surface diffractometer.¹¹ The synchrotron X-ray beam was monochromated to a wavelength of $\lambda = 1.336 \text{ \AA}$. The dimensions of the incoming X-ray beam on the liquid surface were approximately $5 \times 50 \text{ mm}^2$. For the GID experiments, the X-ray beam was adjusted to strike the surface at an incident angle of $\alpha \approx 0.85\alpha_c$, where α_c is the critical angle for total external reflection.¹² Such a geometrical configuration maximizes surface sensitivity.¹³

The monolayers were spread from $5 \times 10^{-6} \text{ M}$ 1:9 methanol-chloroform solutions at $21 \text{ }^\circ\text{C}$ onto a thermostated Teflon trough equipped with a Wilhelmy balance and a barrier for surface pressure control. The pressure-area isotherms for each of the compositions studied (0, 1.3, and 9.0 mol % DSPE-PEG) are shown in Figure 1. At high surface pressures, $\Pi > 30 \text{ mN/m}$, the lateral interactions of the polymer chains are not evident in the pressure isotherm, as the polymer chains are completely submerged in the water subphase. As a result, at high surface pressures the measurements are dominated by the headgroup-headgroup interactions and are not sensitive to the lateral polymer-polymer interaction in the subphase. To probe these interactions and to determine if the physical structure of the monolayer was changing with DSPE-PEG content, GID and reflectivity measurements were conducted on mixed monolayers compressed to 42 mN/m which corresponds to an averaged packing area of about 40 \AA^2 per lipid molecule.^{9,14} Previous studies have demonstrated that under these conditions homogeneous monolayers are formed which do not phase separate.⁹ Parameters for the monolayers at 42 mN/m are given in the inset of Figure 1.

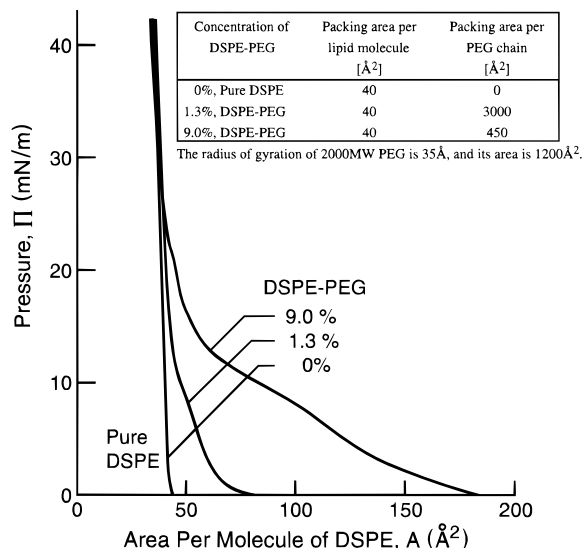


Figure 1. Monolayer compression (Π -A) isotherms of mixed DSPE/DSPE-PEG at $21 \text{ }^\circ\text{C}$. The area, A, is the mean area per molecule at the air-water interface. At high surface pressures ($\Pi > 30 \text{ mN/m}$) the lateral interactions of the polymer chains are not evident in the pressure isotherm, as the polymer chains are completely submerged in the water subphase. Inset: parameters for the PEG polymer grafting density.

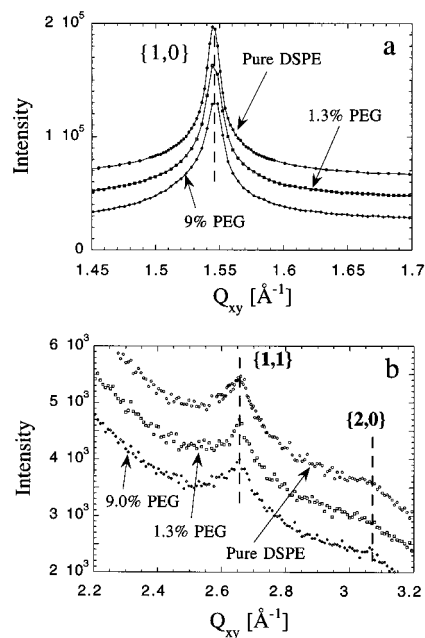


Figure 2. The GID Q_x -integrated diffraction peaks of pure DSPE lipid and DSPE/DSPE-PEG mixed monolayers. For clarity $\{1,0\}$ reflections (shown in a) were displaced by 4000 and the high order $\{1,1\}$ and $\{2,0\}$ reflection (shown in b) by 500 counts, respectively.

Three in-plane reflections: $\{1,0\}$, $\{1,1\}$, and $\{2,0\}$ (Figure 2) are observable from the GID data for pure DSPE and mixed DSPE/DSPE-PEG monolayers. All three compositions studied, 0, 1.3, and 9.0% DSPE-PEG, have at an applied pressure of 42 mN/m the same hexagonal unit cell dimension of $a_H = 4.70$

(14) The DSPE (MW = 747) and DSPE-PEG (i.e., the PEG lipid, MW = 2747) were purchased from Avanti Polar Lipids. They were $>99\%$ pure. The PEG had a molecular weight of 2000 (i.e., 45 monomers) and a polydispersity of 1.1. The subphase consisted of Millipore purified H_2O , $\Omega = 18.2$. Although the solubility of DSPE-PEG ($6 \times 10^{-6} \text{ M}$) is significantly greater than unmodified DSPE ($1 \times 10^{-12} \text{ M}$), the monolayers were very stable (no loss of surface area) over the time course of the X-ray measurements.

(8) Cevc, G.; Hauser, M.; Kornyshev, A. A. *Langmuir* **1995**, *11*, 3103–3110. Cevc, G.; Hauser, M.; Kornyshev, A. A. *Langmuir* **1995**, *11*, 3111–3118.

(9) Kuhl, T. L.; Leckband, D. E.; Lasic, D. D.; Israelachvili, J. N. Modulation and modeling of interaction forces between lipid bilayer exposing terminally grafted polymer chains. In *Stealth Liposomes*; Lasic, D., Martin, F. Eds; CRC Press: Boca Raton, FL, 1995; pp 73–91. Majewski, J.; Kuhl, T. L.; Gerstenberg, M.; Israelachvili, J. N.; Smith, G. S. *J. Phys. Chem.* **1997**, *101*, 3122.

(10) Szleifer, I.; Carignano, M. A. Tethered polymer layers. In *Advances in Chemical Physics*; Prigogine, I., Rice, S. A., Eds.; John Wiley and Sons: New York, 1996; Vol. XCIV, pp 165–259. Alexander, S. *J. Phys. (Paris)* **1977**, *38*, 983. de Gennes, P. G. *Macromolecules* **1980**, *13*, 1069. Milner, S.; Witten, T.; Cates, M. *Macromolecules* **1988**, *21*, 2610.

(11) Majewski, J.; Popovitz-Biro, R.; Bouwman, W. G.; Kjaer, K.; Als-Nielsen, J.; Lahav, M.; Leiserowitz, L. *Chemistry – A European Journal* **1995**, *1*, 304.

(12) In this case the critical angle for total external reflection for the water subphase is $\alpha_c = 0.14^\circ$.

(13) Eisenberger, P.; Marra, W. C. *Phys. Rev. Lett.* **1981**, *46*, 1081.

Table 1. Box Model Parameters Used To Fit the X-ray Reflectivity Data in Figure 5c

composition	σ (Å)	T parabola (Å)	e density start parabola ^a	e density head A layer ^a	T head A layer (Å)	e density head B layer ^a	T head B layer (Å)	e density tail ^a	T tail (Å)	χ^2
1.3% PEG	3.70	34.8	1.01	1.46	4.70	1.34	4.31	0.95	20.40	15.4
9.0% PEG	4.42	48.0	1.06	1.39	5.47	1.17	5.00	0.85	18.03	19.8

^a Electron density divided by electron density of water subphase.

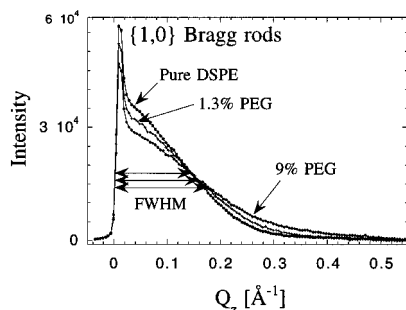


Figure 3. The Bragg rod intensity profiles of the $\{1,0\}$ reflection of the pure DSPE lipid and DSPE/DSPE-PEG monolayers. The sharp peak at $Q_z = 0.01 \text{ \AA}^{-1}$ (Vineyard–Yoneda peak²⁴), arises from the interference between X-rays diffracted up into the Bragg rod and rays diffracted down and then reflected back up by the interface.

Å, and thus the same repeat distance of $d_{10} = 4.07 \text{ \AA}$ and a constant area per lipid molecule of 38.3 \AA^2 . However, the widths of the $\{1,0\}$ Bragg peaks in Figure 2 increase with DSPE–PEG concentration indicating that the size of two-dimensional crystallites decrease as more and more polymer–lipid molecules are introduced. Quantitatively, using the Scherrer formula,¹⁵ we find that the crystallite size is 360 \AA for pure DSPE and it decreases to 280 \AA (230 \AA) for 1.3% (9%) DSPE–PEG concentration.

Figure 3 shows the Bragg rods of the $\{1,0\}$ reflections.¹⁶ Evidently the width of the Bragg rods increases systematically with increasing DSPE–PEG concentration. This means that the length, normal to the water surface, of Bragg scattering moieties of the lipid molecules, gets shorter. One possibility could be that the molecules tilt more and more, thereby obtaining a shorter projection onto the surface normal. However, the detailed shape of the Bragg rods depends on the tilt, and by fitting to a simple model of cylindrically symmetric and longitudinally uniform lipid tails,^{1,17} we find a constant tilt angle of $t = 4 \pm 0.5^\circ$ for all three concentrations. The observed increase in the width of the Bragg rods is therefore due to shorter and shorter portions of the molecules Bragg scattering. A very plausible model for this effect is depicted in Figure 4. With increasing DSPE–PEG concentration, the vertical position of

(15) Guinier, A. *X-ray Diffraction*; Freeman: San Francisco, 1968. Equation 5.3. The in-plane coherence length is the average length, in the direction of the reciprocal lattice vector Q_{hk} , of all diffracting 2D crystallites over which “perfect” crystallinity extends.

(16) In general, monolayers composed of crystallites on the water surface are azimuthally randomly oriented and so may be described as “2-D powders”. Thus, the collection of the diffracted radiation using a position sensitive detector which intercepted photons over the range $0.0 \leq Q_z \leq 0.9 \text{ \AA}^{-1}$ was made in two ways. The scattered intensity was measured by scanning over a range along the horizontal scattering vector $Q_{xy} \approx 2k \sin(\theta_{xy})/\lambda$, (where $k = 2\pi/\lambda$ and $2\theta_{xy}$ is the angle between the incident and diffracted beam projected onto the horizontal plane) and integrated over the whole Q_z window of the position sensitive detector (PSD), to yield the Bragg peaks. Simultaneously, the scattered intensity recorded in channels along the PSD, but integrated over the scattering vector in the horizontal plane across a Bragg peak, produces Q_z -resolved scans called Bragg rod profiles.

(17) Kjaer, K.; Als-Nielsen, J.; Helm, C. A.; Laxhuber, L. A.; Möhwald, H. *Phys. Rev. Lett.* **1987**, *58* (21), 2224. Helm, C. A.; Tippman-Krayer, P.; Möhwald, H.; Als-Nielsen, J.; Kjaer, K. *Biophys. J.* **1991**, *60*, 1457. Helm, C. A.; Möhwald, H.; Kjaer, K.; Als-Nielsen, J. *Biophys. J.* **1987**, *52*, 381.

the molecules becomes less and less ordered, and the tail end, as well as the tail part nearest to the head, therefore get space for lateral disorder and therefore do not Bragg scatter. This model is in keeping with the chemical nature of the DSPE–PEG lipids. Compared to pure unmodified DSPE, the DSPE–PEG lipids have a very bulky, hydrophilic headgroup composed of phosphatidyl ethanolamine terminated by a 2000 MW methoxy-PEG chain. Because PEG is a water-soluble polymer, the DSPE–PEG lipids have a greater solubility than unmodified DSPE, as evidenced by a critical micellar concentration of $6 \times 10^{-6} \text{ M}$ compared to $1 \times 10^{-12} \text{ M}$.¹⁸ This increased solubility should naturally result in a higher density of protrusions from the monolayer interface into the water subphase.⁹ Similarly, the increase in size of the DSPE–PEG headgroup might be expected to increase the lateral spacing of the lipids in the monolayer, but as shown above this does not take place: the dimension of the unit cell is unaffected by the DSPE–PEG concentration. A quantitative analysis of the width of the Bragg rods reveals that the length of the coherently diffracting lipid tails decrease from 23 \AA for pure DSPE to 20 \AA and 18 \AA for 1.3% and 9.0% DSPE-PEG, respectively.¹⁹

The Bragg scattering gives only information about the laterally ordered parts of the molecules, e.g., the middle part of the lipid tails. We could not detect any direct evidence in the GID data of where the PEG portion of the DSPE-PEG molecules is located. However, this information can be obtained from specular X-ray reflectivity. Figure 5a shows the reflectivity data for 1.3 and 9.0 mol % DSPE–PEG in the DSPE layer. The observed reflectivities have been normalized to the Fresnel reflectivity R_F for an ideal, infinitely sharp air–liquid interface with the electron density of water in the liquid phase.¹ We initially fit the reflectivity data using a free-form fitting routine,²⁰ and the corresponding electron density profiles are shown in Figure 5b. From these free-form profiles several observations can be made. First, the polymer layer extension into the water subphase and its integrated electron density increase with higher DSPE–PEG concentration. At the same time, it is also evident that the electron density of the headgroup and tail regions with 9.0% DSPE–PEG is less than that determined for 1.3% DSPE–PEG.

Next, we analyzed the reflectivity data using model-dependent fits. The lipid monolayer was modeled by boxes.²¹ In the case of 9.0% DSPE–PEG, we found that it was necessary to divide the headgroup region into two boxes to improve the quality of

(18) It has been previously demonstrated that the polymer chains do not penetrate the monolayer, but extend away from the headgroup region into the subphase. Hence, only the presence of air in the tail region of the monolayer can account for its apparent decrease in the scattering density. In other words, a simple Gaussian smearing of the interface does not represent the staggered structure of the monolayer properly in our model.

(19) The out-of-plane Debye–Waller factor used to fit Bragg rod data was $1.0\text{--}1.5 \text{ \AA}$. Our Bragg rod analysis did not require different out-of-plane Debye–Waller factors for the different concentrations of PEG lipid (the Q_z extension of the $\{1,0\}$ Bragg rods was only about 0.3 \AA^{-1}).

(20) Pedersen, J. S.; Hamley, I. W. *J. Appl. Crystallogr.* **1994**, *27*, 36.

(21) To numerically approximate the electron density profile of the system, several small slabs (each $\sim 0.5 \text{ \AA}$ thick) were used. The values of the reflectivity were calculated using these slabs and χ^2 was minimized in a Marquardt–Levenburg nonlinear least-squares fitting routine to obtain the best fitting parameters.

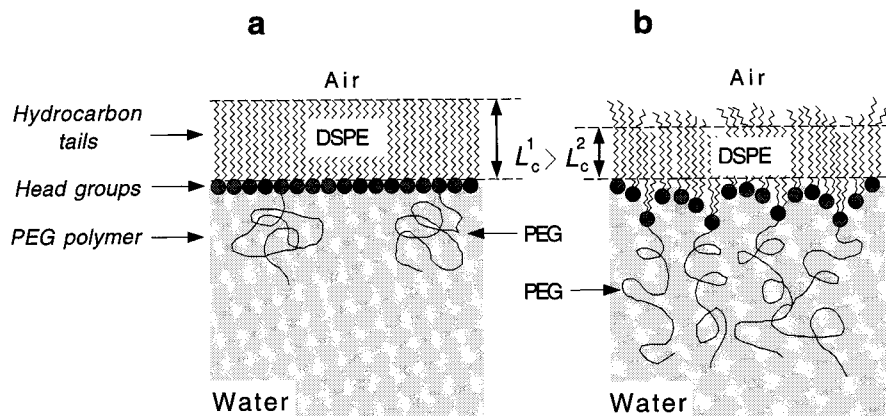


Figure 4. Schematic structure of a mixed DSPE/DSPE-PEG monolayer showing the decrease in length of the coherently scattering lipid tails due to the greater out of plane protrusions of the DSPE-PEG molecules from the 2D plane of the monolayer, where L_c is the coherently scattering length.

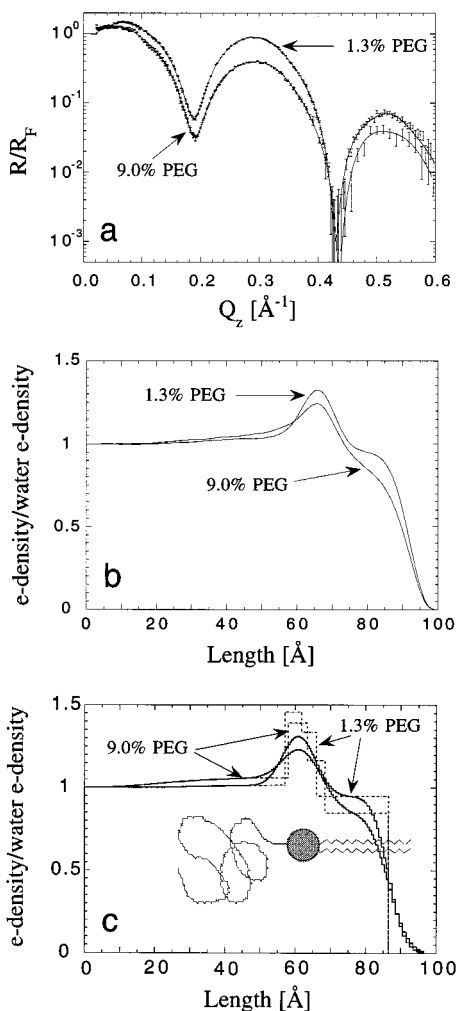


Figure 5. (a) X-ray reflectivity data, the solid lines are fits to the data using a free-form fitting routine.²⁰ (b) The corresponding normalized electron density profiles obtained from the free-form fittings. (c) The normalized electron density profiles obtained by fitting the model discussed in the text (parameters shown in Table 1). For easy reference a schematic of a single DSPE-PEG lipid is shown to scale with the fitted electron density profiles.

the fit.⁷ An additional box was used to describe the lipid tail region. Although the electron densities of PEG and water are not very different²² and the concentration of PEG is quite small, it was necessary to include a polymer layer in order to obtain a reasonable fit to the reflectivity data, even at the low

concentration of 1.3% DSPE-PEG. In other words, by specular reflectivity data one could “see” the PEG part of the film. Moreover, at the higher 9.0% DSPE-PEG concentration, the polymer layer was best modeled by a parabolic function.²³ The resulting electron density profiles and fitting parameters are shown in Figure 5c and Table 1. The length of the parabola at 1.3% DSPE-PEG, 35 Å, matches very well with the expected, $R_F = 35$ Å, and previously measured thickness of 35 Å.⁹ The higher concentration of 9.0% DSPE-PEG required a longer parabola of 48 Å with a higher electron density. Finally, the electron density ratio of 8.2 integrated over the length of the parabolas is in good agreement with the actual molar ratio of 7.0 PEG.

However, the fitting of the 9.0% DSPE-PEG reflectivity data proved to be problematic. The model-independent fitting clearly indicated that the electron density of the lipid monolayer, head and tail region, decreased with increasing DSPE-PEG concentration. Our model-dependent fits also had this trend. Although we believe that this is due to the increased protrusions of the lipid monolayer at the higher DSPE-PEG concentration, we were unable to properly account for this staggered structure using simple models i.e., with boxes while maintaining the calculated total number of electrons per square angstrom in the lipid monolayer to that known from the chemical formula (Table 1). At present we have no explanation for this.

In summary, we have determined that lipids with bulky hydrophilic polymer headgroups have large fluctuations normal to the monolayer plane, resulting in a systematic roughening of the interface and a decrease in the coherently Bragg-scattering tail thickness with increasing polymer-lipid content. These results suggest that bulky hydrophilic moieties cause significant out-of-plane protrusions of phospholipid monolayers and presumably bilayers, vesicles, and biological membranes. The results further indicate that in-plane or lateral packing stresses (due to bulky hydrophilic polymer-lipid headgroups) can be relaxed predominately through an increase in out of plane protrusions and not by increasing the area occupied per molecule.

(22) The electron density of bulk PEG is only 6% higher than the water subphase.

(23) Due to the weak contrast between the polymer and subphase, the 1.3% DSPE-PEG reflectivity data could be reasonably well fit with a simple box of constant e density to describe the polymer layer and thus was not sensitive to the functional form of the polymer profile. However, at 9.0% DSPE-PEG a simple box for the polymer did not fit the data, while a parabolic form did. Specifically, the polymer layer was modeled with a concave parabola with decreasing density from the monolayer interface.

(24) Vineyard, G. *Phys. Rev. B.* **1982**, 26, 4146.

Acknowledgment. We gratefully acknowledge beamtime at HASYLAB at DESY, Hamburg, Germany, and funding by the programs DanSync (Denmark) and TMR (European Union). This work was partially supported by the U.S. Department of Energy under contract W-7405-ENG-36, the Department of

Energy (DOE) under Grant DE-FG03-87ER45331, and by the MRL Program of the National Science Foundation under Award No. DMR-9123048.

JA973024N